NASA TECHNICAL MEMORANDUM

NASA TM X-71717

NASA TM X-71717

(NASA-TM-X-71717) THE AERODYNAMIC DESIGN OF A COMPRESSOR-DRIVE TURBINE FOR USE IN A 75 kw AUTOMOTIVE ENGINE (NASA) 39 p HC $3.75 CSCL 21A

N75-21633

Unclas G3/37 18665

THE AERODYNAMIC DESIGN OF A COMPRESSOR-DRIVE TURBINE FOR USE IN A 75 KW AUTOMOTIVE ENGINE

by Richard J. Roelke and Kerry L. McLallin
Lewis Research Center
Cleveland, Ohio 44135

April 1975

ABSTRACT

The design of a single stage axial-flow turbine with a tip diameter of 11.15 cm is presented in this report. The design specifications are given and the aerodynamic design procedure is described. The aerodynamic information reported includes the results of flow path, velocity diagram, and blade profile studies. Predicted off-design performance characteristics are also presented.

SUMMARY

The Energy Research and Development Agency (ERDA) is conducting a program to demonstrate a gas turbine powered automobile that meets the 1978 Federal Emissions Standards with acceleration characteristics and fuel economy that are competitive with current conventionally powered vehicles. In part, the program consists of designing a new gas turbine engine for a compact passenger vehicle to meet the program objectives. The turbomachinery components for the new or "upgraded" engine have been designed at the Lewis Research Center. The aerodynamic design of the compressor-drive turbine is presented herein.

The compressor-drive turbine is a single stage axial flow design. It is similar in configuration to the compressor-drive turbine of the existing sixth generation or "baseline" gas turbine manufactured by the Chrysler Corporation. However, the engine mass flow has been reduced to 0.598 Kg/s, which is 60% of the baseline value, and the turbine inlet temperature was increased from the baseline value of 1283 to 1325 K. The work factor was reduced from 2.5 in the baseline turbine to 2.1 in the "upgraded" turbine, which could result in an improvement in efficiency. A turbine total efficiency estimate of 0.85 was used for the design. The "upgraded" turbine has a radius ratio of 0.7973 and a tip diameter of 11.15 cm.

INTRODUCTION

The Energy Research and Development Agency (ERDA) is conducting a program to demonstrate a gas turbine powered automobile that meets the 1978 Federal Emissions Standards with acceleration characteristics and fuel economy that are competitive with current conventionally powered vehicles. Part of this program involves an evaluation of mid-size passenger vehicles powered by the existing sixth generation gas turbine manufactured by the Chrysler Corporation. Another part of the program consists of the design of a new engine for a smaller vehicle to meet the emission objective of the program with a significant improvement in vehicle fuel economy.

The existing or "baseline" gas turbine engine delivers 112 KW in a 2000 Kg vehicle. The new or "upgraded" gas turbine engine will deliver 75 KW in a 1600 Kg vehicle with the capability of brief power augmentation to 90 KW through the use of variable guide vanes and water injection at the compressor inlet. Improved fuel economy of the upgraded engine and vehicle will result from the reduced vehicle size and vehicle power-to-weight ratio, and possible improvements in component efficiencies.

The turbomachinery components for the "upgraded" engine have been designed at the Lewis Research Center. These include the compressor, the compressor-drive turbine, the power turbine, the duct between the turbines, and the turbine exit diffuser. The aerodynamic design of the compressor-drive turbine is presented herein. The aerodynamic designs of the compressor and power turbine are detailed in references 1 and 2, respectively. Also included in reference 2 are the transition duct and exit diffuser designs.

This report contains the design specifications of the compressor-drive turbine and a description of the aerodynamic design procedure.

The aerodynamic information includes the results of the flow path and velocity diagram studies, the approach taken in the development of the blade profiles, and off-design performance estimates.

SYMBOLS

A	blade profile cross-sectional area, cm^2
B	blade trailing edge blockage, $TET/s \cos \alpha_{b,ex}$
C	blade chord, cm
D_s	suction surface diffusion, $1 - W_{ex}/W_{s,max}$
D_p	pressure surface diffusion, $1 - W_{p,min}/W_{in}$
Δh	specific work, J/kg
h	blade height, cm
P	pressure, N/cm^2
r	radial distance from axis of rotation, cm
R_{st}	stator reaction, $1 - (V_0/V_1)^2$
R_{ro}	rotor reaction, $1 - (W_1/W_2)^2$
s	blade pitch, cm
TET	blade trailing edge thickness, cm
U	blade speed, m/s
V	absolute fluid velocity, m/s
w	mass flow, kg/s
W	fluid velocity relative to blade, m/s
X	axial coordinate, cm
Y	tangential coordinate, cm
α	absolute flow angle, deg
β	flow angle relative to blade, deg
γ	specific heat ratio
δ	ratio of turbine inlet to U.S. standard sea level atmospheric pressure, $P_0'/10.1325$

ϵ specific heat ratio equivalence parameter $.7396/\left[\gamma_0\left(\frac{2}{\gamma_0+1}\right)^{\gamma_0/(\gamma_0-1)}\right]$

η efficiency

θ squared ratio of turbine inlet to U.S. standard sea level atmosphere critical velocity, $(V_{cr,0}//a_{10.64})^2$

ψ coefficient of aerodynamic loading, see App. B of reference 7

Ω turbine wheel speed, rad/s

Subscripts:

b condition inside flow channel at blade inlet or exit

CR conditions at Mach 1

des design point

eq equivalent condition

ex blade exit

h hub

in blade inlet

m mean

max maximum value

min minimum value

p pressure surface

s suction surface

t tip

0 axial station at stator inlet (figure 1)

1 axial station at stator exit or rotor inlet (figure 1)

2 axial station at rotor exit (figure 1)

Superscript:

' total condition

DESIGN SPECIFICATIONS

The aerodynamic design of the upgraded compressor-drive turbine is not markedly different from the baseline machine. Both turbines are small single stage axial flow machines. The design conditions of the upgraded turbine are listed in Table I. These design conditions are similar to the baseline engine conditions with two exceptions. The design gas flow of the baseline turbine was 1.015 kg/s compared to 0.598 kg/s for the upgraded turbine. Also the turbine inlet temperature of the upgraded turbine was increased from the baseline turbine value of 1283 to 1325 K.

For reasons of component packaging, mechanical design and engine response time several design constraints were imposed on the aerodynamic design. These constraints are listed in Table II. The work factor ($\Delta h/U_m^2$) was 2.5 and 2.1 for the baseline and upgraded turbines, respectively. It was estimated that this decrease in work factor of the upgraded turbine would correspond to about a one point improvement in efficiency. Another point increase in efficiency could result by reducing the work factor to 1.8. However, as this parameter is reduced the turbine diameter and polar amount of inertia increase, increasing the engine response time to a gas pedal change. Consideration of these opposing factors by the ERDA lead to the selection of a 2.1 work factor design. A single stage axial flow design was mandated so that the packaging of the upgraded components would be similar to that of the baseline engine. The stator inlet angles were specified to match the swirl distribution in the tangential entry

inlet manifold. The remaining constraints listed in Table II, with the exception of the roto.' trailing edge blockage, were selected for mechanical and fabrication reasons. An upper limit of rotor trailing edge blockage was specified to preclude a large aerodynamic loss at the rotor exit.

FLOW PATH AND VELOCITY DIAGRAMS

The upgraded compressor-drive turbine was designed with a constant mean diameter of 10.008 cm and cylindrical (i.e., no flare) hub and tip endwalls. The turbine flow path in the radial-axial plane is shown in figure 1. The rotor tip was recessed in the casing .012 cm beyond the stator tip radius. The rotor tip radial clearance was fixed at .0254 cm which is 2 1/4 percent of the blade height. The hub and tip radii were determined so that the blade hub centrifugal stress did not exceed 16900 N/cm^2.

With this flow path geometry and the design conditions specified in Table I, the design point performance was analyzed using the computer program described in reference 3. This program computes the turbine velocity diagrams for a given set of design requirements, and specified meridional velocity gradients at the stator and rotor exits. The program calculates the turbine efficiency based on a correlation of stator and rotor losses. The calculated efficiency may be modified by specifying multiplying factors for the stator and rotor losses. Since the loss correlation in the computer program is more applicable for turbines that are considerably larger in size than the subject turbine, a separate assessment of the turbine efficiency was made.

Two separate estimates of turbine efficiency were made. The experimental data correlated by Smith, reference 4, was used for one estimate. The base value of efficiency from this reference was adjusted downward after estimating the effect of tip leakage, Reynolds number, and turbine size. The adjusted efficiency was .858. The second estimate of turbine

efficiency utilized the loss data presented in reference 5 and the equations of reference 6. The total efficiency calculated by this method was .841. Based on these two estimates an efficiency of .85 was selected for the turbine and appropriate loss multipliers were coded into the turbine design program.

For the flow path geometry and total efficiency selected, a series of design velocity diagrams were calculated. In this design, the off-design performance was equal in importance to the design performance since the gas turbine engine must operate economically over a range of conditions from engine idle to the design output of 75 KW. Therefore, once an acceptable velocity diagram was obtained at the design speed, turbine performance calculations were made at 50 percent turbine speed (this corresponds to the engine idle condition). Of prime importance was to minimize the turbine exit swirl at the design condition while maintaining a high efficiency with little or no static pressure increase across the rotor hub at engine idle. The final design velocity diagrams are given in figure 2. These velocity diagrams reflect all aerodynamic losses except the tip clearance loss. A tabulation of the final values of swirl, efficiency and rotor reaction for the 75 KW and engine idle conditions is given in Table III. The stage reaction, defined as the ratio of relative kinetic energy change across the rotor to specific work, was 36 percent.

STATOR AND ROTOR BLADE DESIGN

STATOR

A series of calculations were undertaken to choose the stator axial chord at the hub, mean, and tip sections. With the stator blade number being set by manufacturing considerations at 15 blades, the flow channel exit angles and throat dimensions necessary to meet the design velocity diagrams were calculated. Basic stator geometry parameters, such as spacing, throat, and inlet and exit angles, were used to develop a series of layouts at hub, mean, and tip. Stator blade layouts were chosen to minimize axial chord while giving sufficient guided channel between stator blades. The resulting solidities were 1.123, 1.103, and 1.084 at the hub, mean, and tip respectively. The optimum solidities, based on the information in reference 7, range from 1.18 to 1.38. The blade loading coefficients, ψ , at the hub, mean and tip were .568, .664, and .745 respectively.

The stator profiles were developed by an iterative procedure incorporating the use of two computer programs. One of the programs used is described in reference 8. This program, TSONIC, calculates the two-dimensional flow field between adjacent profiles. One of the input variables needed for this program is the variation in stream sheet thickness from inlet to exit. The second computer program, CHANEL, described in reference 9, was used to determine accurately the stream sheet thickness inside the blade channel. This program also provides a three-dimensional continuity check. The procedure followed was to calculate the stator surface velocities at the hub, mean, and tip with TSONIC, initially assuming a linear variation in

stream sheet thickness. The stator profile was then altered, if needed, and the surface velocities recomputed until a smooth transition in surface velocity resulted with a minimum of suction surface diffusion. CHANEL was then used with these profiles to calculate an accurate variation in the stream sheet thickness, which in turn was then used in TSONIC in place of the initially assumed linear variation. The surface velocities calculated with TSONIC using the nonlinear variation in stream sheet thickness were used to make any subsequent changes to the profiles. This iteration process was repeated until a satisfactory surface velocity distribution was obtained. The final stator blade profiles and coordinates are given in figure 3. The surface velocities are shown in figure 4, and a summary of the stator aerodynamic design is presented in Table IV.

ROTOR

The rotor axial chords at hub, mean, and tip were determined by selecting a hub section blade loading coefficient, ψ , of 0.85, which is slightly higher than that recommended in reference 7. The higher loading parameter was chosen to reduce the axial chord and blade number. A range of axial chords and corresponding blade numbers were calculated. A blade number of 56 was selected. The blade loading, ψ , was increased to 0.90 at the tip to insure adequate blade taper in the final configuration. The axial chords at hub, mean, and tip were 1.100, 1.029, and 0.957 cm respectively. Finally, the leading and trailing flow channel angles, velocities, and throat dimensions were calculated at hub, mean, and tip. Using the minimum allowable trailing edge thickness, a hub trailing edge blockage of 11.4 percent was calculated.

The design procedure followed to develop the blade profiles is similar to that used in designing the stator profiles. Initial TSONIC calculations at the hub section indicated a choked condition, at the inlet, for blade angles equal to or greater than the relative inlet gas angle. Small decreases in the inlet blade angle (resulting in positive incidence) relieved the choking problem and also improved the blade surface velocity distributions. However, this change in inlet blade angle added to the positive incidence at other turbine operating conditions, and in particular at idle, which was considered important. To minimize rotor loss due to incidence at the hub, the maximum amount of positive incidence permitted with minimum loss was estimated using the procedure described in reference 10. A maximum positive incidence of 7 degrees was calculated. Between the design and idle conditions the positive incidence at the hub increased by approximately 3 degrees. Therefore, only hub sections having 4 degrees or less positive incidence were considered. The final hub section had +3 degrees incidence at design conditions and therefore +6 degrees incidence at idle. The mean and tip sections had zero and -2 degrees incidence at design conditions respectively. The final rotor blade profiles and coordinates are shown in figure 5 and the surface velocity distributions are given in figure 6. A summary of the rotor aerodynamic design characteristics is presented in Table V. It should be noted that the sections labeled "hub" and "tip" in Table V and figure 5 are nominal hub and tip sections. The exact radii of the hub, mean, and tip sections are 4.445, 5.010, and 5.575 cm (see figure 1).

OFF-DESIGN PERFORMANCE ESTIMATES

As noted in the preceding sections, the turbine off-design performance was utilized in the design of the compressor-drive turbine. These off-design calculations were obtained with the computer program described in reference 11. Calculations were made for rotor speeds from 50 to 100 percent of the design speed and for a range of total-to-total pressure ratios up to 2.6. The results of these calculations are given in figure 7 in terms of the equivalent conditions. The parameters plotted are specific work ($\Delta h/\theta$) and weight flow ($w\sqrt{\theta}\epsilon/\delta$) versus the total-to-total pressure ratio, and efficiency (η') versus the work factor ($\Delta h/U_m^2$). The design and idle conditions are shown on these plots.

REFERENCES

1. Galvas, Michael R.: Compressor Design for the (ERDA) Automotive Gas Turbine Program. NASA TM X-71719, 1975.
2. Kofskey, Milton G.; Katsanis, Theodore; and Schumann, Lawrence F.: Aerodynamic Design of a Free Power Turbine for a 75 KW Gas Turbine Automotive Engine. NASA TM X-71714, 1975.
3. Carter, A. F.; and Lenherr, F. K.: Analysis of Geometry and Design-Point Performance of Axial-Flow Turbines Using Specified Meridional Velocity Gradients. NASA CR-1456, 1969.
4. Smith, S. F.: A Simple Correlation of Turbine Efficiency. Journal of the Royal Aeronautical Society, Vol. 69; July, 1965.
5. Holeski, D. E.; and Stewart, W. L.: Study of NASA and NACA Single-Stage Axial Flow Turbine Performance as Related to Reynold's Number and Geometry. ASME Transactions, July 1964.
6. Stewart, W. L.: A Study of Axial-Flow Turbine Efficiency Characteristics in Terms of Velocity Diagram Parameters. ASME Paper No. 61-WA-37, 1961.
7. Miser, James W.; Stewart, Warner L.; and Whitney, Warren J.: Analysis of Turbomachine Viscous Losses Affected by Changes in Blade Geometry. NACA RM E56F21, 1956.
8. Katsanis, Theodore: Fortran Program for Calculating Transonic Velocities on a Blade-to-Blade Stream Surface of a Turbomachine. NASA TN D-5427, 1969.
9. Katsanis, Theodore: Fortran Program for Quasi-Three-Dimensional Calculation of Surface Velocities and Choking Flow for Turbomachine Blade Rows. NASA TN D-6177, 1971.

10. Ainley, D. G.; and Mathieson, G. C. R.: An Examination of the Flow and Pressure Losses in Blade Rows of Axial-Flow Turbines. ARC Technical Report, R&M No. 2891, 1955.

11. Flagg, E. E.: Analytical Procedure and Computer Program for Determining the Off-Design Performance of Axial Flow Turbines. NASA CR-710, 1967.

TABLE I

TURBINE DESIGN CONDITIONS

	ENGINE CONDITION	EQUIVALENT CONDITION
Inlet Temperature, K	1325	288.15
Inlet Pressure, N/cm^2 abs	39.75	10.13
Mass Flow, kg/s	0.598	0.335
Rotative Speed, rad/s	6126.1	2898.5
Power, KW	118.2	14.84
Specific Work, J/kg	198119	44351.7

TABLE II

DESIGN CONSTRAINTS

Work factor, $\Delta h/U_m^2$	2.1
Single stage axial flow	-----
Stator inlet gas angles, degrees	
hub	52.0
mean	48.7
tip	45.6
Rotor radial tip clearance, cm	.0254
Rotor taper ratio, A_h/A_t	1.5
Minimum trailing edge thickness, cm	.0381
Maximum blade centrifugal stress, N/cm^2	16900
Number of stator blades	15
Maximum rotor t.e. blockage, B	.15

TABLE III

COMPARISON OF SELECTED VELOCITY DIAGRAM PARAMETERS AT ENGINE DESIGN AND IDLE CONDITION

	ENGINE DESIGN	ENGINE IDLE
Inlet temperature, K	1325	1114
Inlet pressure, N/cm^2 abs	39.75	14.78
Rotative speed, rad/s	6126.1	3063.1
Pressure ratio, p_0^i/p_2^i	1.94	1.23
Total efficiency, η'	.85	.858
Exit swirl, deg	-21.1	-19.9
Rotor hub static pressure ratio, $(P_{1,h}/P_{2,h})$	1.173	1.0
Rotor hub reaction, $R_{ro,h}$	.207	-.185

TABLE IV

COMPRESSOR DRIVE TURBINE STATOR DESIGN PARAMETERS

	HUB	MEAN	TIP
PROFILE RADIUS, r, cm	4.445	5.004	5.563
AXIAL CHORD, cm	1.067	1.168	1.270
CHORD, C, cm	2.091	2.311	2.525
PITCH, s, cm	1.862	2.096	2.330
SOLIDITY, C/s	1.123	1.103	1.084
THROAT, cm	0.740	0.841	0.928
PROFILE CROSS-SECTIONAL AREA, A, cm^2	.265	.271	.329
LEADING EDGE RADIUS, cm	.0635	.0635	.0635
INLET BLADE ANGLE, deg	50.1	46.7	43.6
INCIDENCE, deg	-2.0	-2.0	-2.0
TRAILING EDGE RADIUS, cm	0.0191	0.0191	0.0191
EXIT BLADE ANGLE, deg	65.5	65.2	65.5
TRAILING EDGE BLOCKAGE, B	0.050	0.043	0.040
REACTION, R_{st}	.822	.813	.800
AERODYNAMIC LOADING, ψ	.568	.664	.745
SUCTION SURFACE DIFFUSION, D_s	.020	.029	.031
PRESSURE SURFACE DIFFUSION, D_p	.029	.116	.168
BLADE NUMBER		15	
TAPER RATIO, A_h/A_t		0.804	
BLADE HEIGHT, h, cm		1.118	
ASPECT RATIO, h/C_m		0.484	
RADIUS RATIO, r_h/r_t		.799	

TABLE V

COMPRESSOR DRIVE TURBINE ROTOR DESIGN PARAMETERS

	HUB	MEAN	TIP
PROFILE RADIUS, r_s, cm	4.458	5.010	5.563
AXIAL CHORD, cm	1.100	1.0287	0.957
CHORD, C, cm	1.104	1.043	.9907
PITCH, s, cm	0.5002	0.5621	.6242
SOLIDITY, C/s	2.207	1.856	1.587
THROAT, cm	0.2952	.3186	.3408
PROFILE CROSS-SECTIONAL AREA, A, cm^2	.1368	.1100	.0931
LEADING EDGE RADIUS, cm	.0356	.0331	.0305
INLET BLADE ANGLE, deg	49.13	45.73	39.62
INCIDENCE, deg	+3.0	0	-2.0
TRAILING EDGE RADIUS, cm	0.0191	0.0191	0.0191
EXIT BLADE ANGLE, deg	-48.22	-50.61	-52.63
TRAILING EDGE BLOCKAGE, B	0.114	0.107	0.101
REACTION, R_{ro}	.217	.537	.725
AERODYNAMIC LOADING, ψ	.866	.889	.908
SUCTION SURFACE DIFFUSION, D_s	.151	.174	.158
PRESSURE SURFACE DIFFUSION, D_p	.52	.515	.509
BLADE NUMBER		56	
TAPER RATIO, A_h/A_t		1.47	
BLADE HEIGHT, h, cm		1.13	
ASPECT RATIO, h/C_m		1.08	
RADIUS RATIO, r_h/r_t		0.797	
TIP CLEARANCE, cm		0.0254	

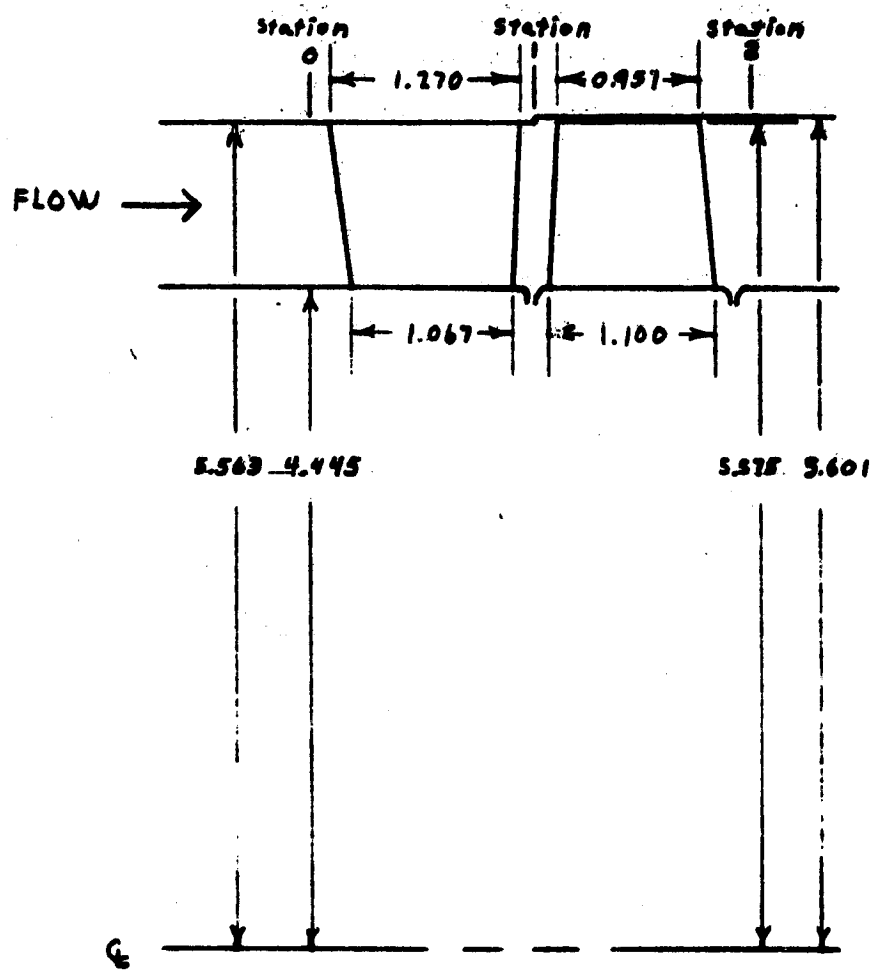

FIGURE 1. COMPRESSOR DRIVE TURBINE FLOW PATH
DIMENSIONS IN CM.

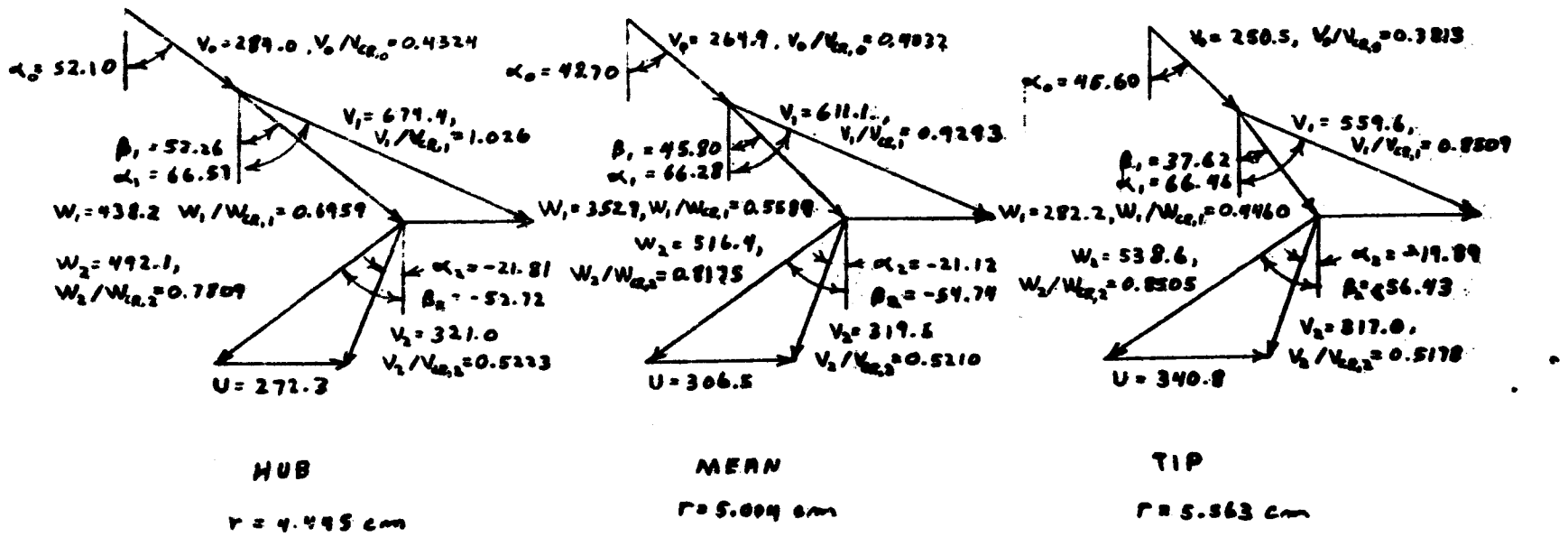

FIGURE 2. COMPRESSOR DRIVE TURBINE DESIGN VELOCITY DIAGRAMS. (velocities in m/s)

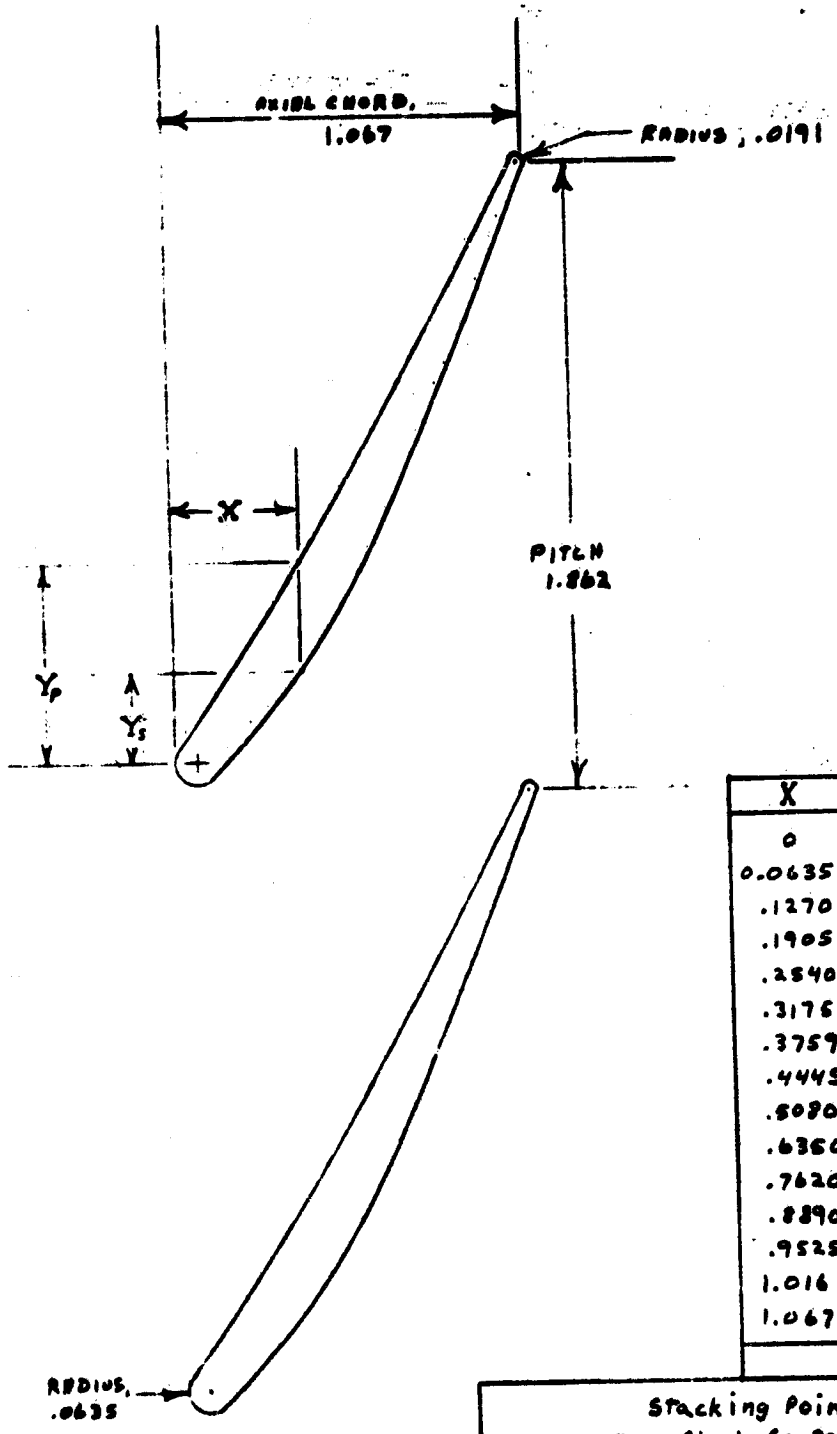

X	Y_s	Y_p
0	0	0
0.0635	-0.0635	0.1100
.1270	-.0269	.2007
.1905	.0394	.2959
.2540	.1080	.3937
.3175	.1836	.4940
.3759	.2604	-
.4445	.3569	.7015
.5080	.4623	.8115
.6360	.7187	1.036
.7620	1.013	1.266
.8890	1.322	1.509
.9525	1.483	1.627
1.016	1.645	1.754
1.067	1.775	1.775

	X	Y
Stacking Point	0.0635	0
Leading Edge Circle Center	.0635	0
Trailing Edge Circle Center	1.048	1.775

a. HUB, r = 4.445

FIGURE 3. COMPRESSOR-DRIVE TURBINE STATOR PROFILES AND COORDINATES. (Dimensions in cm.)

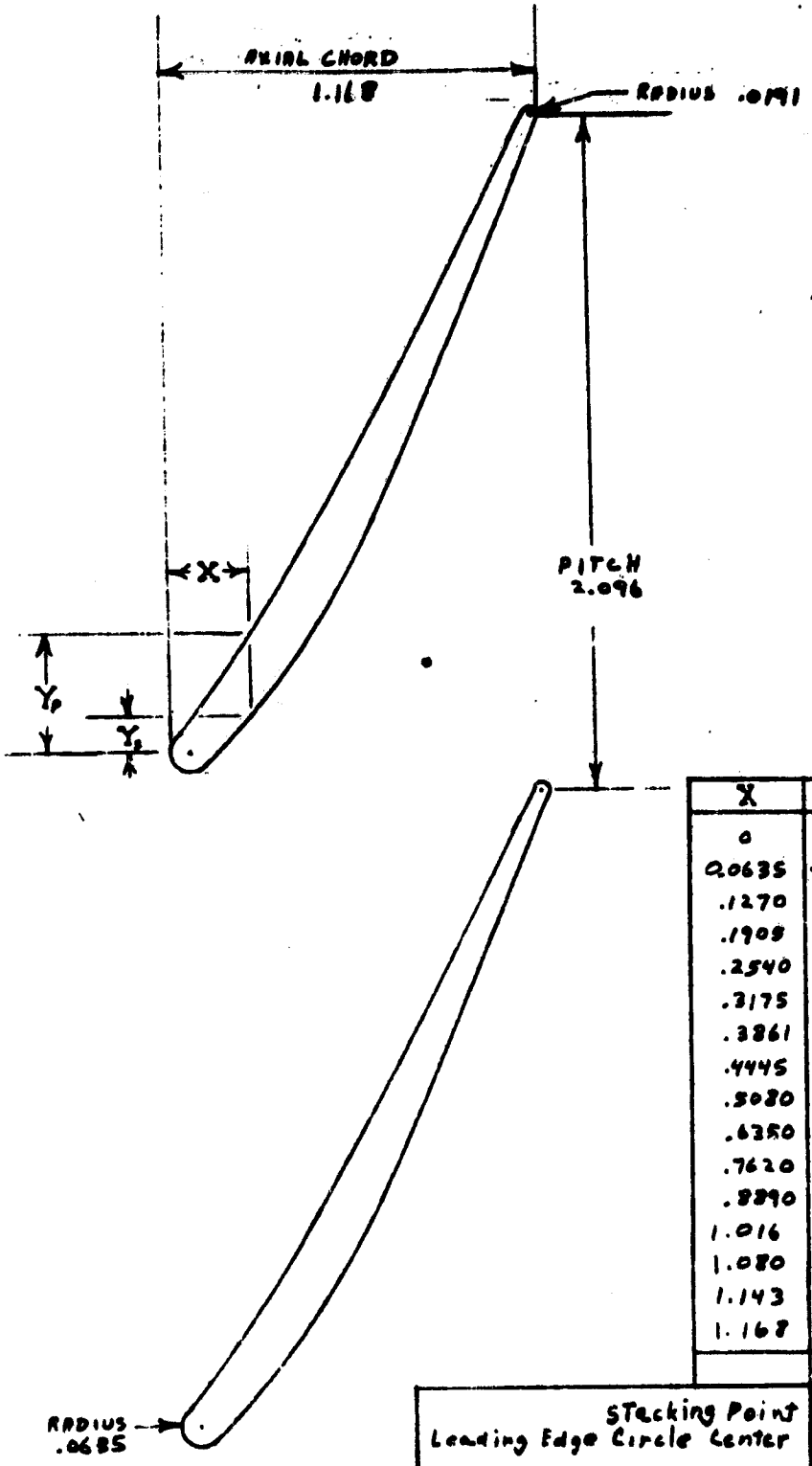

X	Y_s	Y_p
0	0	0
0.0635	-0.0389	0.0973
.1270	-.0279	.1839
.1909	.0351	.2710
.2540	.1041	.3632
.3175	.1765	.4618
.3861	.2700	-
.4445	.3569	.6718
.5080	.4648	.7849
.6350	.7097	1.017
.7620	.9890	1.255
.8890	1.280	1.502
1.016	1.591	1.748
1.080	1.746	1.872
1.143	1.901	1.986
1.168	1.969	1.969

	X	Y
Stacking Point	0.1549	0.0869
Leading Edge Circle Center	.0635	0
Trailing Edge Circlecenter	1.149	1.969

b. MEAN, r_c 6.004

Fig 3

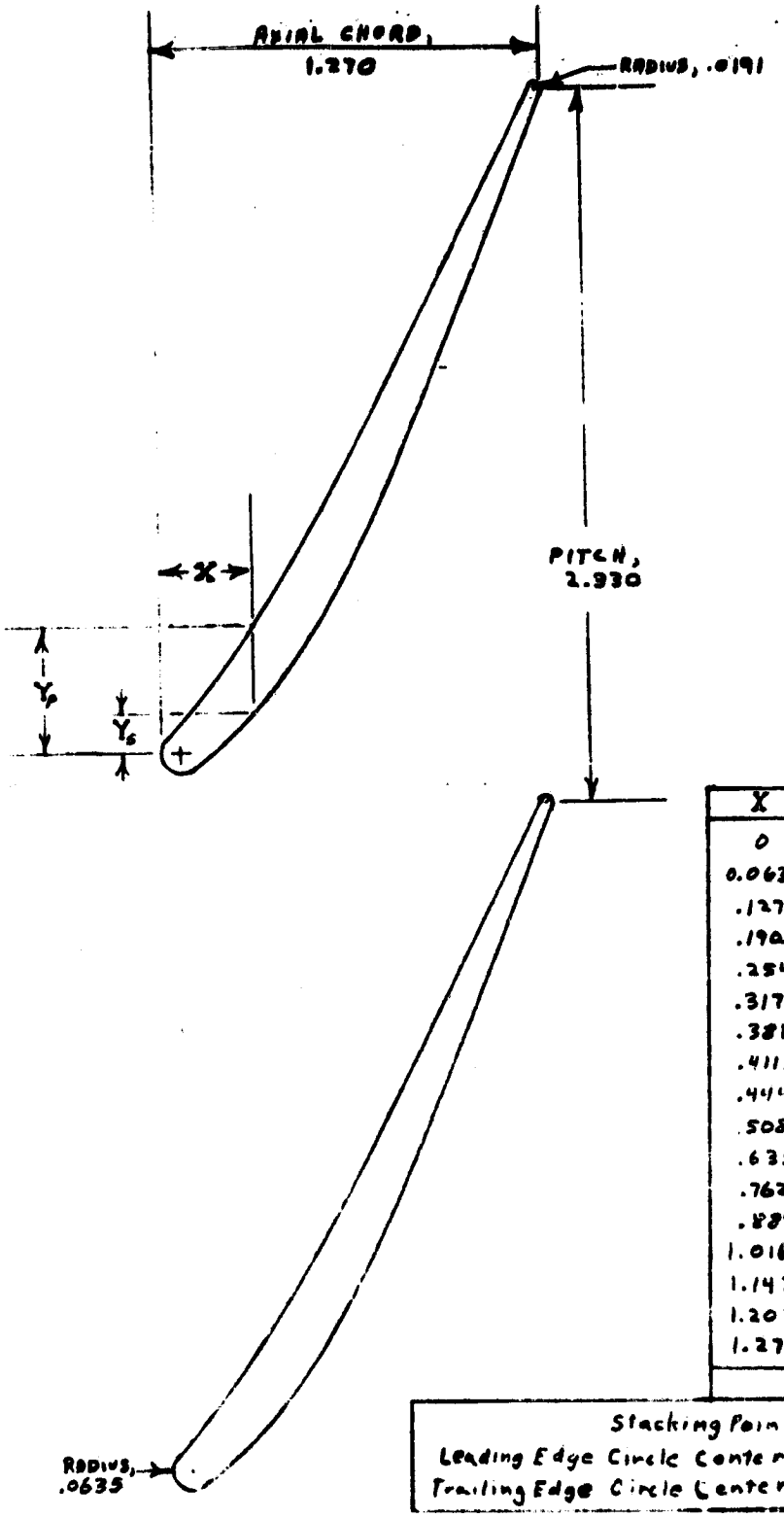

X	Y_s	Y_p
0	0	0
0.0635	-0.0685	0.0953
.1270	-.0305	.1715
.1905	.0231	.2548
.2540	.0828	.3444
.3175	.1488	.4407
.3810	.2225	.5420
.4115	.2629	-
.4445	.3089	.6487
.5080	.4079	.7592
.6350	.6365	.9917
.7620	.9007	1.235
.8890	1.195	1.486
1.016	1.505	1.740
1.143	1.833	1.991
1.207	1.990	2.118
1.270	2.159	2.159

	X	Y
Stacking Point	0.2469	0.1727
Leading Edge Circle Center	.0635	0
Trailing Edge Circle Center	1.251	2.159

C. TIP, r = 3.563

Fig 3.

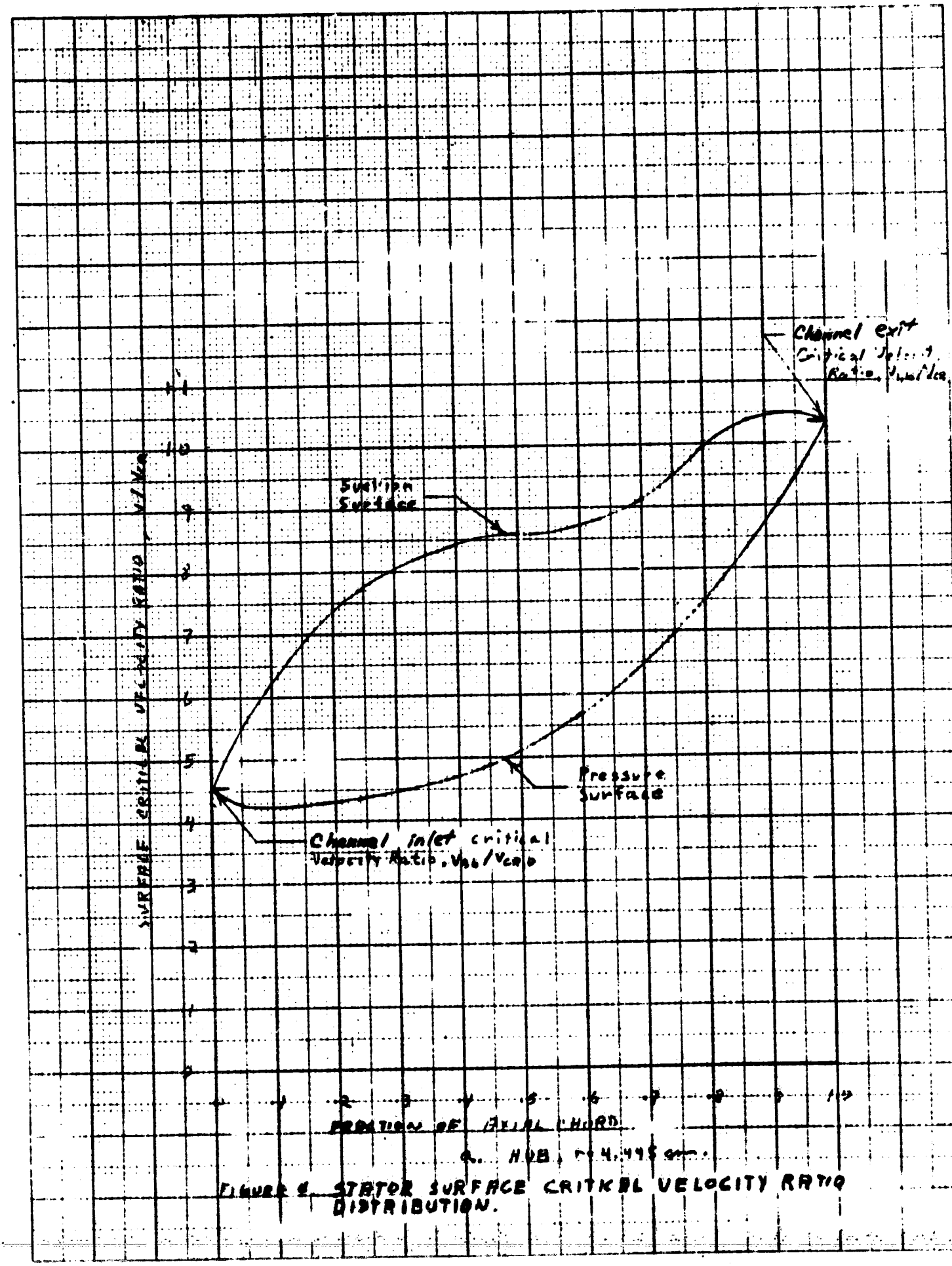

FIGURE 6. STATOR SURFACE CRITICAL VELOCITY RATIO DISTRIBUTION.

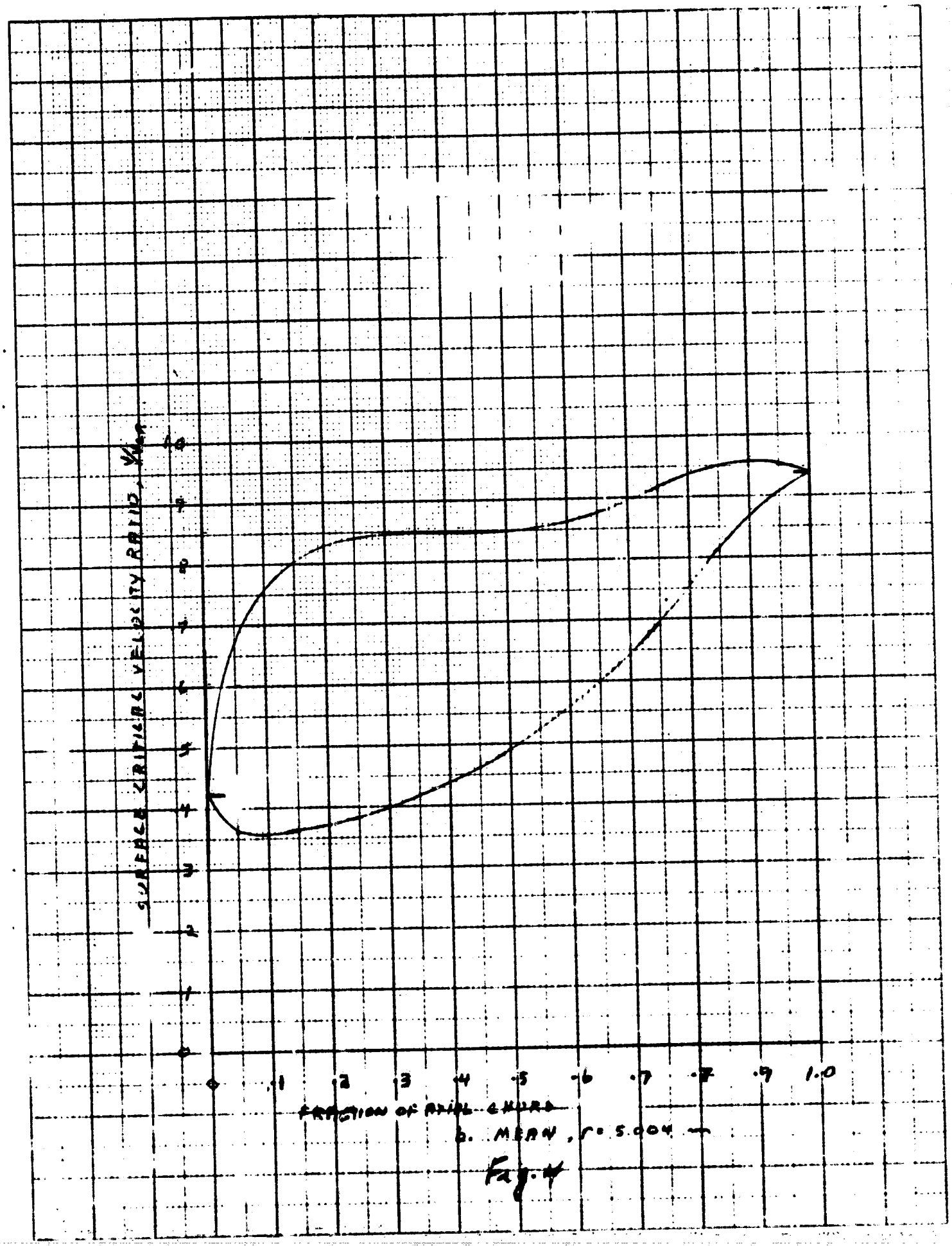
SURFACE CRITICAL VELOCITY RATIO, V_{cr}/V_{mean}
0
1
2
3
4
5
6
7
8
9
10
.1
.2
.3
.4
.5
.6
.7
.8
.9
1.0
FRACTION OF AXIAL CHORD
b. MEAN, r = 5.004 —

Fig. 4

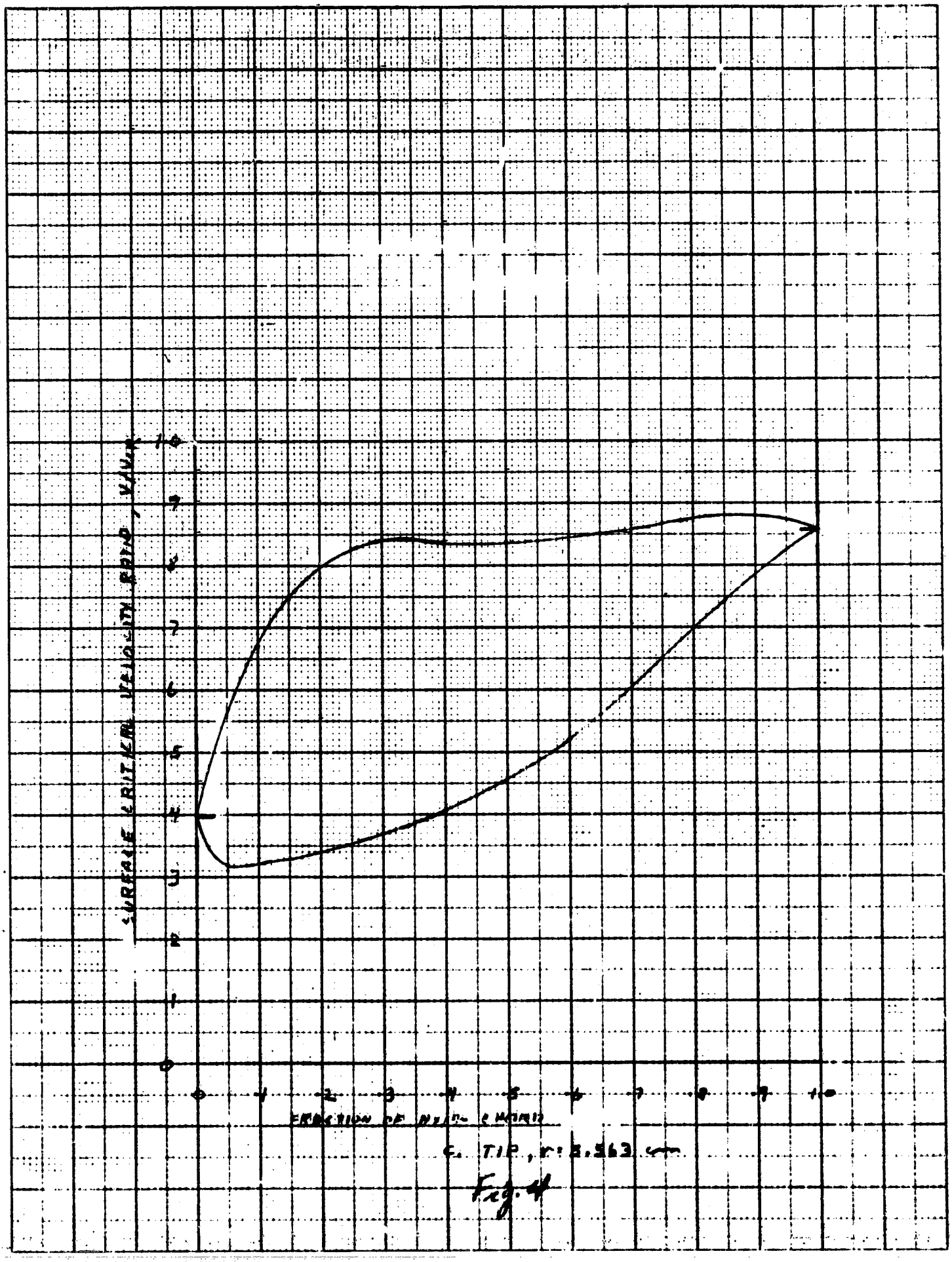

C. T.E., r: 3.563 cm

Fig. 4

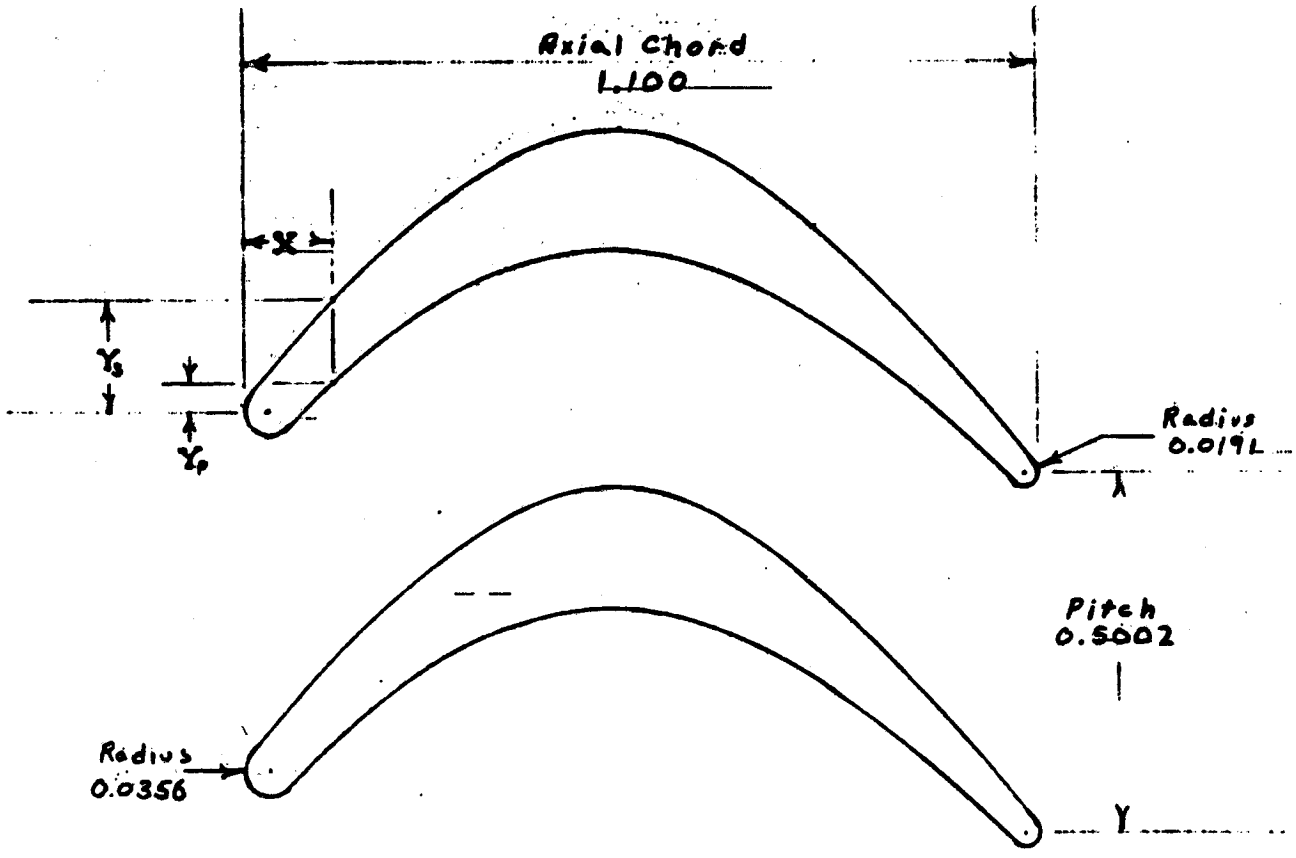

X	Y_s	Y_p	X	Y_s	Y_p
0	0	0	0.60	0.3787	0.2135
0.05	0.0724	-0.0320	.65	.3570	.1988
.10	.1282	.0160	.70	.3270	.1780
.15	.1800	.0623	.75	.2890	.1524
.20	.2265	.1036	.80	.2470	.1222
.25	.2695	.1395	.862	.1875	—
.30	.3080	.1695	.90	.1500	.0495
.35	.3413	.1933	.95	.0970	.0075
.40	.3675	.2106	1.00	.0415	-.0370
.45	.3854	.2210	1.05	-.0185	-.0840
.50	.3940	.2253	1.10	-.0875	-.0875
.55	.3912	.2225			

	X	Y
STACKING POINT	0.5349	0.2026
LEADING EDGE CIRCLE CENTER	.0356	0
TRAILING EDGE CIRCLE CENTER	1.081	-.0875

R. HUB ; r= 4.458

FIGURE 5. COMPRESSOR DRIVE TURBINE ROTOR PROFILES AND COORDINATES. (Dimensions in cm.)

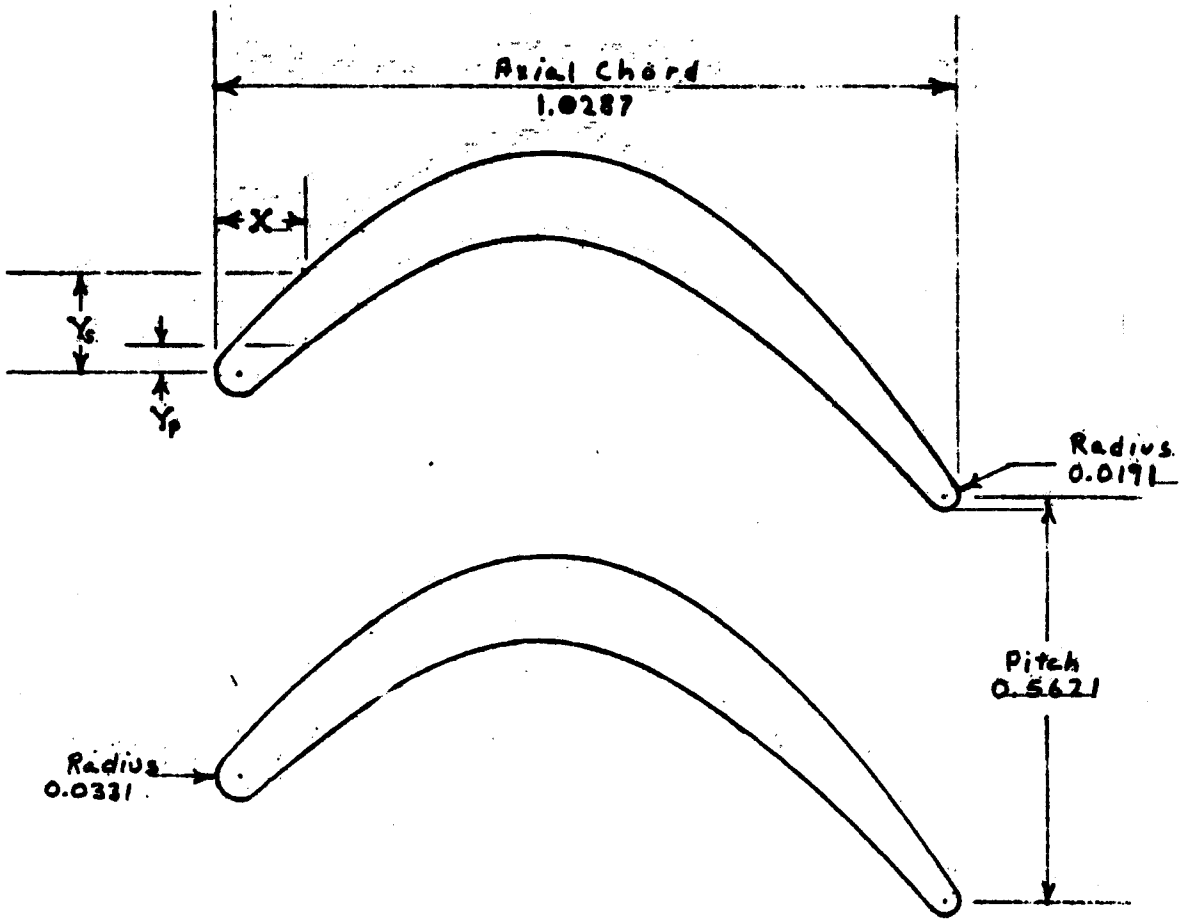

X	Y_s	Y_p	X	Y_s	Y_p
0	0	0	0.60	0.2767	0.1500
0.05	0.0670	-0.0280	.65	.2500	.1223
.10	.1175	.0155	.70	.2142	.0888
.15	.1626	.0570	.75	.1715	.0500
.20	.2028	.0945	.7685	.1550	—
.25	.2375	.1260	.80	.1245	.0076
.30	.2660	.1530	.85	.0700	-.0380
.35	.2874	.1734	.90	.0100	-.0865
.40	.3015	.1855	.95	-.0540	-.1360
.45	.3090	.1900	1.00	-.1235	-.1855
.50	.3060	.1845	1.0287	-.1700	-.1700
.55	.2953	.1710			

	X	Y
STACKING POINT	0.5099	0.1287
LEADING EDGE CIRCLE CENTER	.03305	0
TRAILING EDGE CIRCLE CENTER	1.0097	-.1700

b. MEAN; r = 5.01

Fig 5

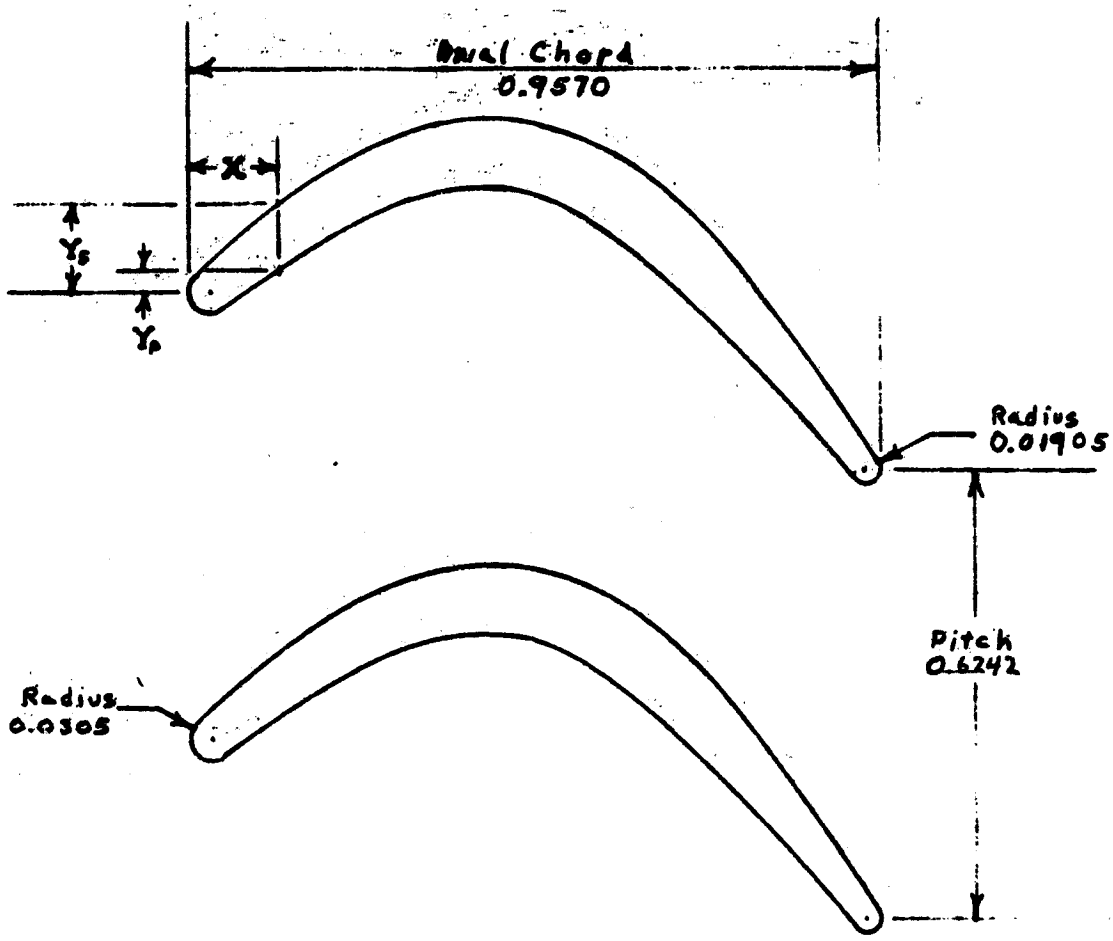

X	Y_s	Y_p	X	Y_s	Y_p
0	0	0	0.55	0.2145	0.1012
0.05	0.0600	-0.0240	.60	.1880	.0670
.10	.1015	.0120	.65	.1523	.0265
.15	.1387	.0465	.67	.1350	—
.20	.1710	.0775	.70	.1055	-.0200
.25	.1987	.1055	.75	.0500	-.0705
.30	.2196	.1264	.80	-.0145	-.1245
.35	.2340	.1400	.85	-.0845	-.1790
.40	.2410	.1460	.90	-.1585	-.2380
.45	.2400	.1426	.957	-.2600	-.2500
.50	.2310	.1270			

	X	Y
STACKING POINT	0.4945	0.0123
LEADING EDGE CIRCLE CENTER	.0305	0
TRAILING EDGE CIRCLE CENTER	.93796	-.2500

C. TIP, r = 5.563

Fig 6

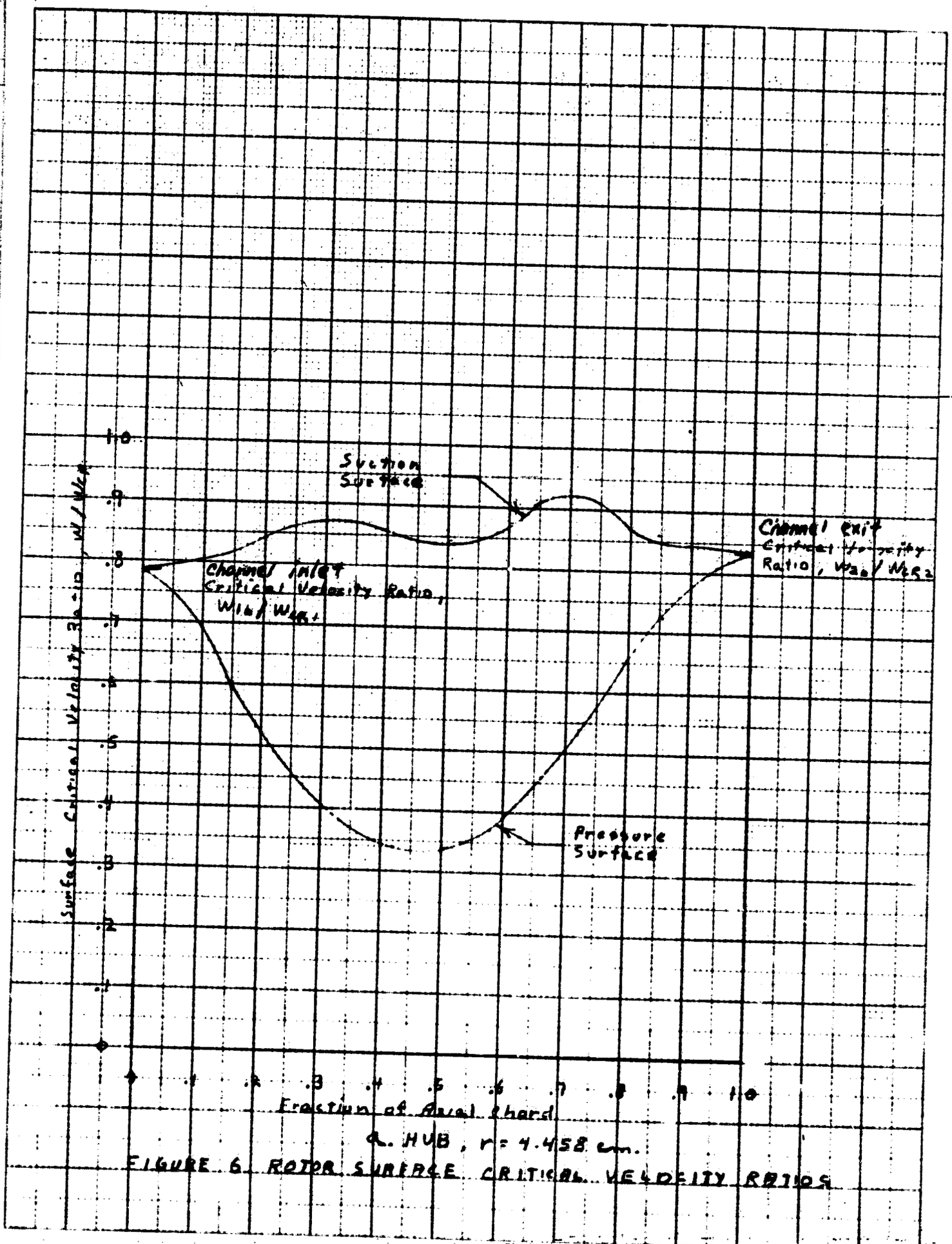

a. HUB, r = 4.458 cm.

FIGURE 6. ROTOR SURFACE CRITICAL VELOCITY RATIOS

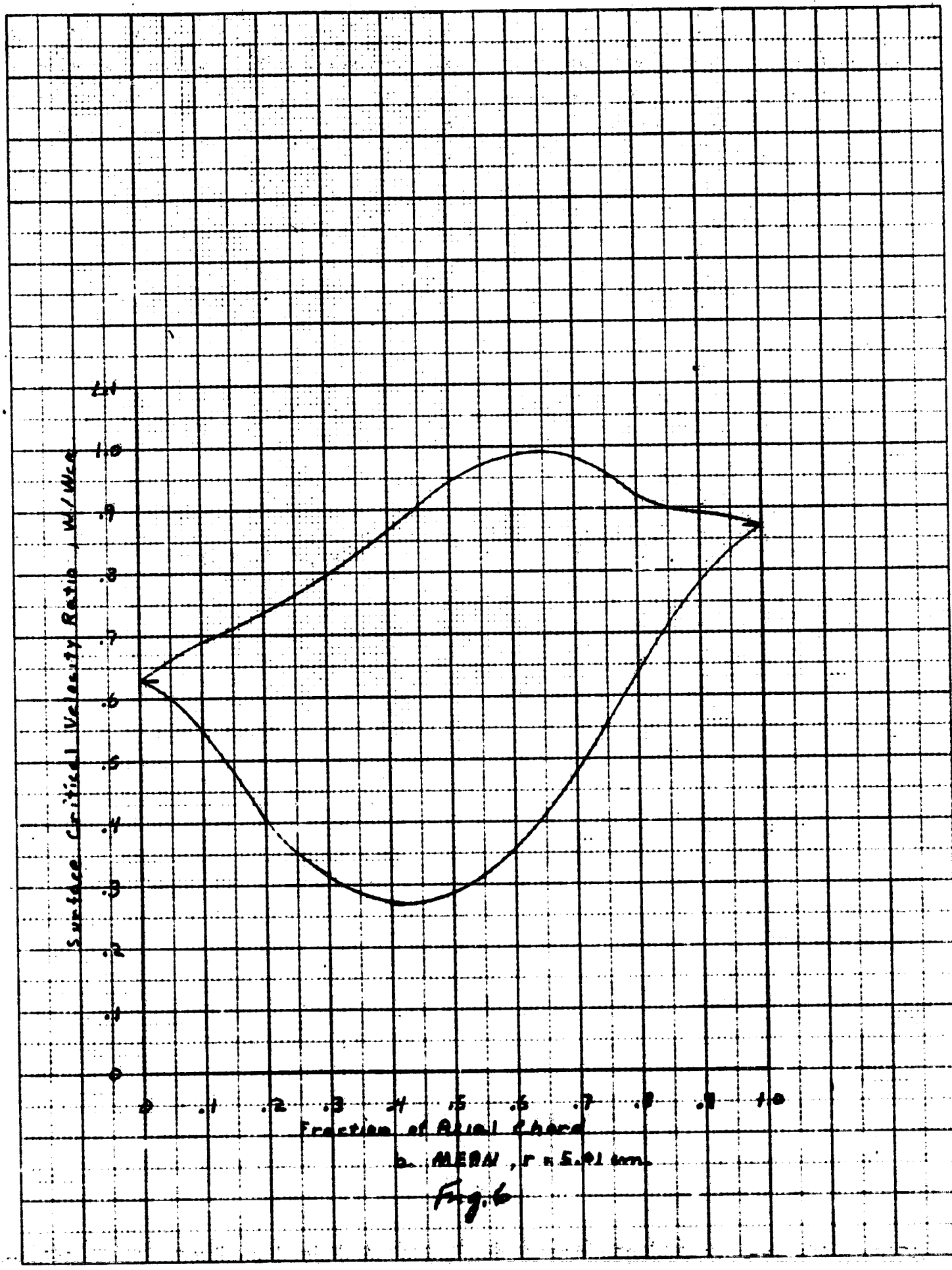

b. MEAN, r = 5.91 mm.

Fig. 6

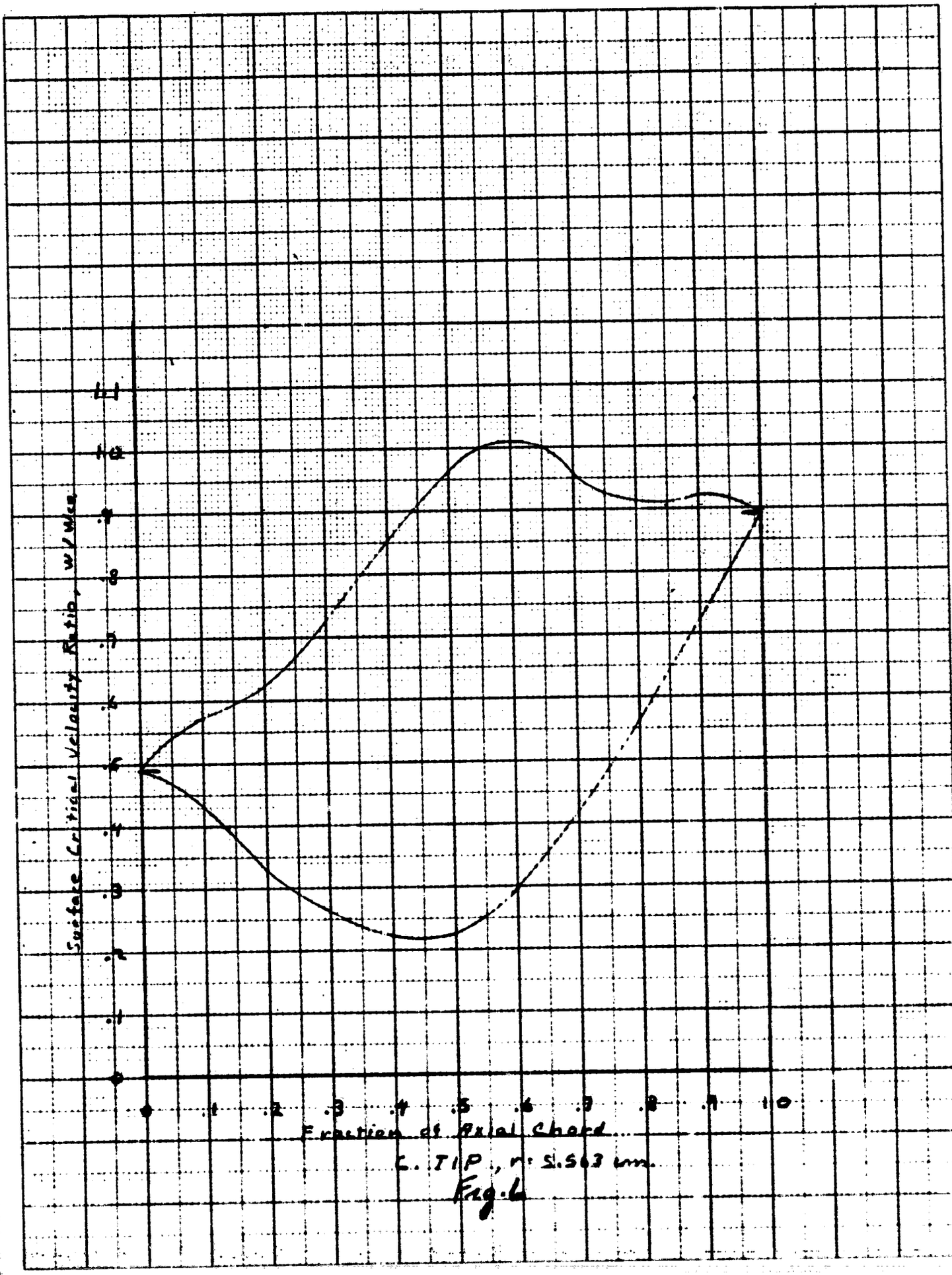
Surface Critical Velocity Ratio, w/w∞
1.1
1.0
.9
.8
.7
.6
.5
.4
.3
.2
.1
0
.1
.2
.3
.4
.5
.6
.7
.8
.9
1.0
Fraction of Axial Chord
L. TIP, r = 5.563 in.

Fig. 4

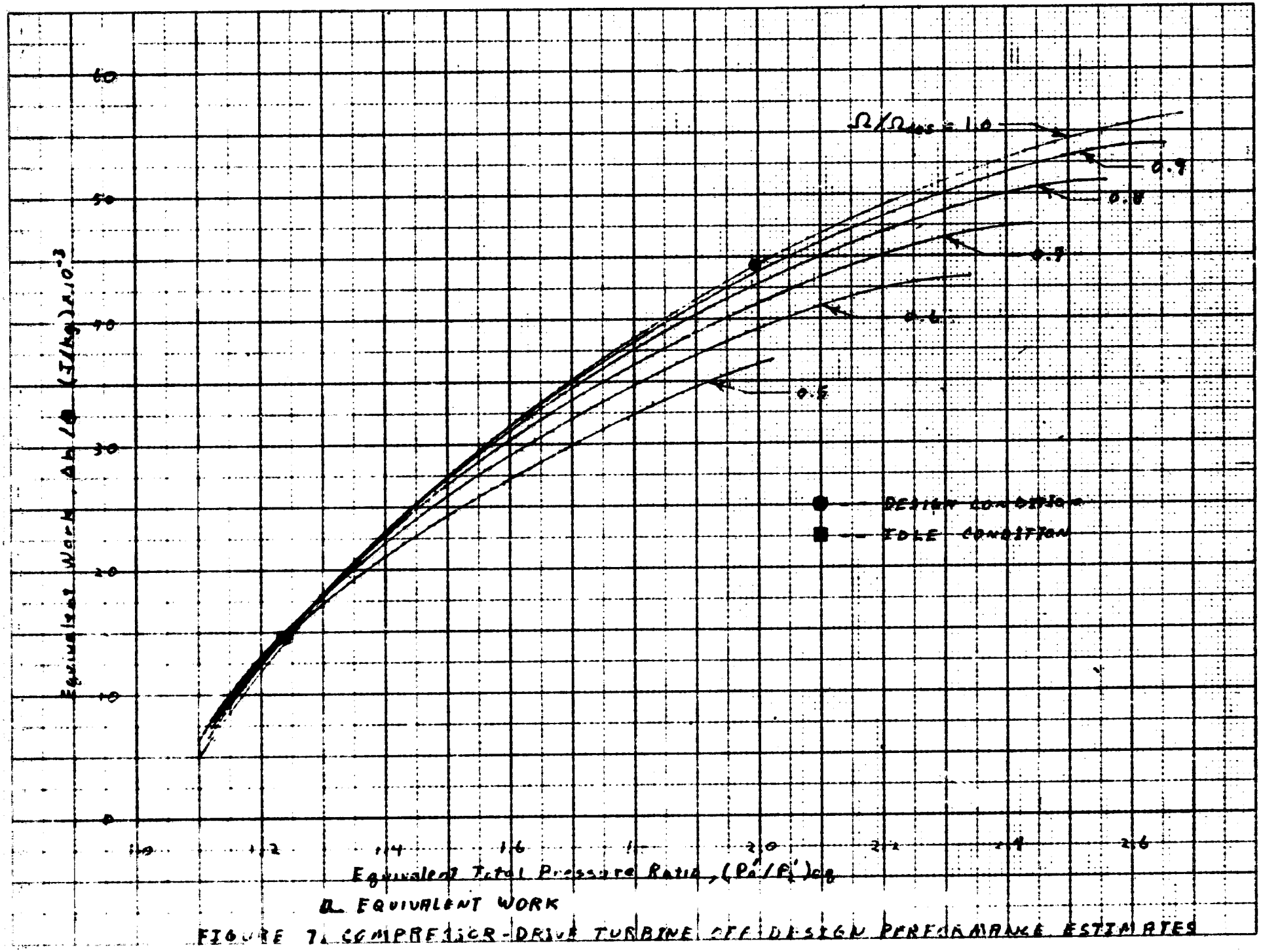

a. EQUIVALENT WORK

FIGURE 7. COMPRESSOR-DRIVE TURBINE OFF-DESIGN PERFORMANCE ESTIMATES

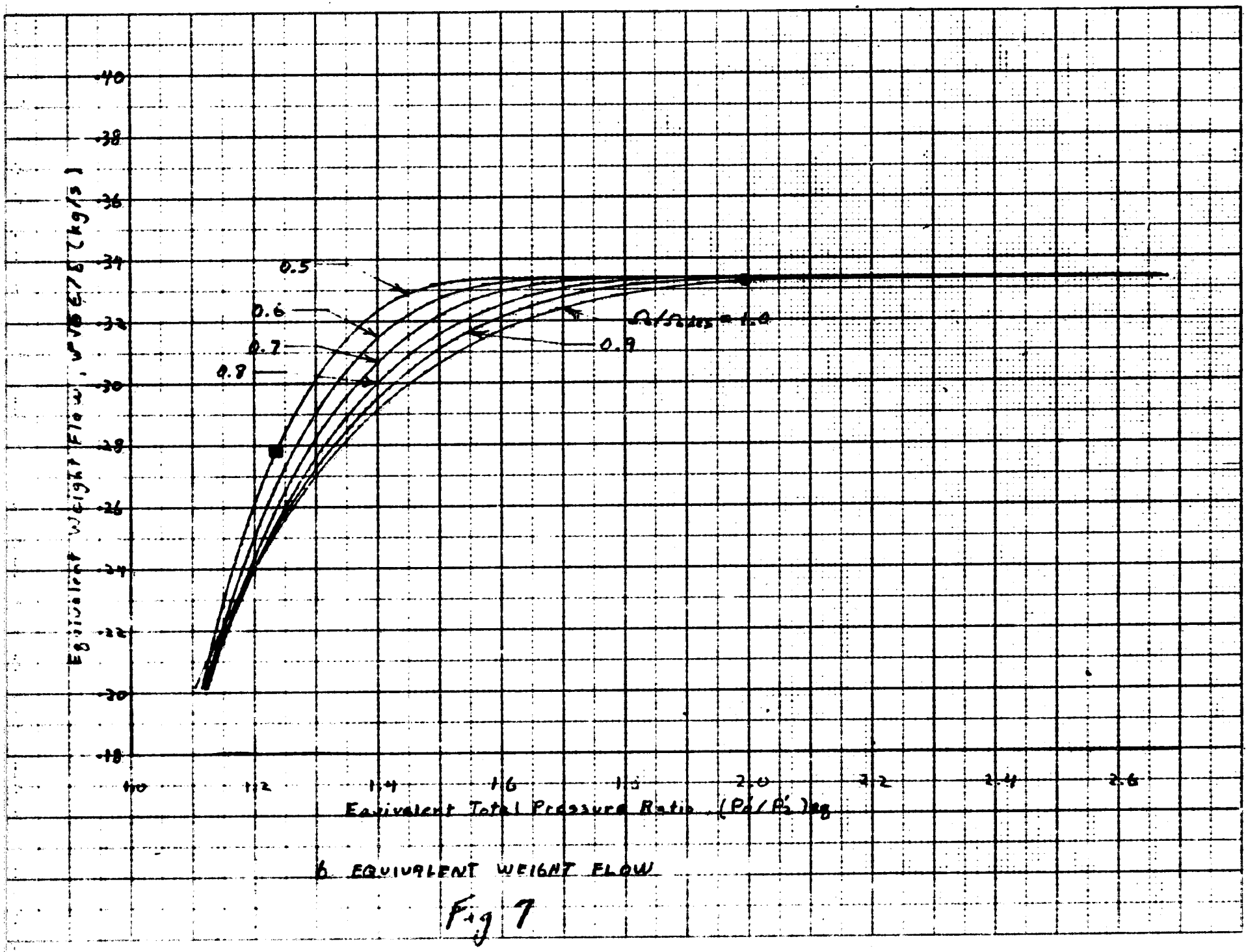

b EQUIVALENT WEIGHT FLOW

Fig 7

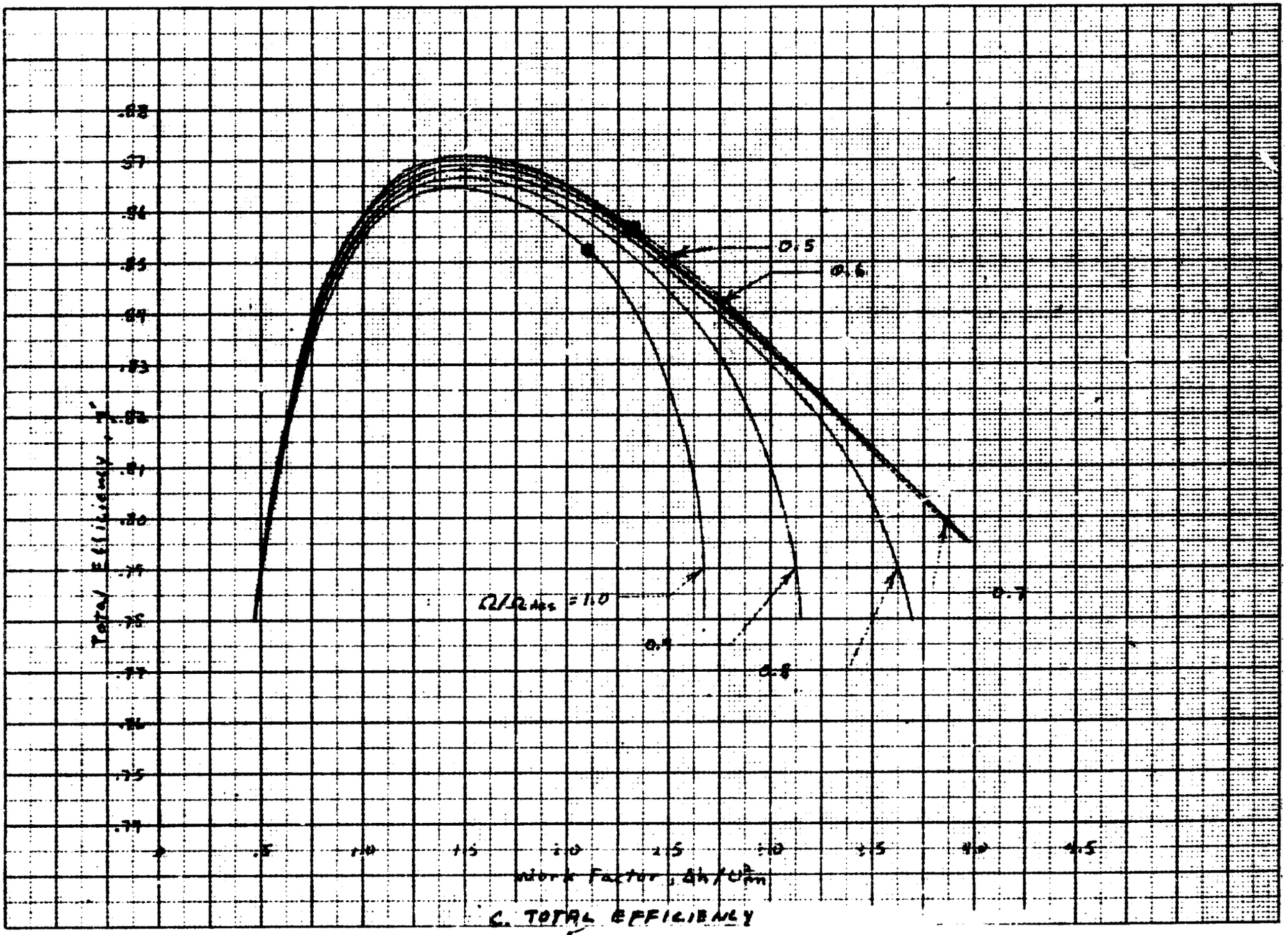

C. TOTAL EFFICIENCY

Fig 7